Unusual neon isotopic composition in Neoproterozoic sedimentary rocks: Fluorine bearing mineral contribution or trace of an impact event?

Deborah Chavrit, Manuel Moreira, David Fike, Frédéric Moynier

Unusual neon isotopic composition in Neoproterozoic sedimentary rocks: fluorine bearing mineral contribution or trace of an impact event?

Déborah Chavrit[1], Manuel A. Moreira[1*], David A. Fike[2], Frédéric Moynier[1,3]

[1] Institut de Physique du Globe de Paris, Sorbonne Paris Cité, Univ Paris Diderot, CNRS, F-75005 Paris, France

[2] Department of Earth and Planetary Sciences, Washington University, St Louis, Missouri 63130, USA

[3] Institut Universitaire de France, Paris, France

* corresponding author

Contacts:

Déborah Chavrit: deborahchavrit@gmail.com

Manuel A. Moreira: Moreira@ipgp.fr

David A. Fike: dfike@levee.wustl.edu

Frédéric Moynier: Moynier@ipgp.fr

Keywords

noble gas; Ediacaran sedimentary rocks; Ne-A; nucleogenic; fluorite; Acraman impact

Highlights

- Helium and neon isotopes have been measured in Huqf supergroup in Oman
- Neon shows a peculiar isotopic signature suggesting either a major extraterrestrial impact or a peculiar enrichment in fluorine

Abstract

Extraterrestrial materials have He and Ne isotopic compositions that are distinct from those of the Earth's surface. In order to track the extraterrestrial material accreted onto Earth during the Ediacaran period, we have analyzed the He and Ne isotopic composition of thirteen sedimentary rocks in the age range ~550-600 Ma, coming from the Huqf supergroup in Oman for which carbon and sulfur isotopic data have been characterized previously.

$^{3}He/^{4}He$ ratios range between 0.006±0.003 and 0.27±0.01 R_A, with R_A being the atmospheric ratio. $^{3}He/^{4}He$ ratios show a positive relationship with ^{3}He contents ranging between 0.6 and 31 $\times 10^{-13}$ cm^3 $STP.g^{-1}$. The ^{3}He contents are within the literature data for 3 to 480 Myr old samples with evidence of IDP ^{3}He (IDP for interplanetary dust particles), suggesting that extraterrestrial ^{3}He is still retained in such old samples.

$^{20}Ne/^{22}Ne$ ratios are close to or below the modern atmospheric ratio of 9.8 with the minimum value equal to 9.05±0.03. $^{21}Ne/^{22}Ne$ ratios show a high range of variation, going from 0.0345±0.0009 to 0.0935±0.0023. The Ne isotopic compositions follow a nucleogenic trend similar to that of crustal fluids from the literature and predicted continental crust. However, one sample (3404) shows an unusual Ne isotopic composition with a lower $^{20}Ne/^{22}Ne$ at similar $^{21}Ne/^{22}Ne$ compared to the other samples.

Two hypotheses can explain this singular Ne isotopic composition. First, it could be the result of a particular nucleogenic trend due to the presence of F-bearing minerals in this sample. SEM-EDS elemental mapping showed that although F- and Ca-rich phases, which could correspond to fluorites, are present in sample 3404. However, their abundance of ~0.15% seem too low to explain the unusual Ne isotopic composition. However, due to the high uncertainty of the calculations, we cannot totally rule out this hypothesis. Alternatively, the singular Ne isotopic composition could be due to the presence of a Ne-A component, a component characterizing pre-solar diamonds contained in chondrites. This would indicate that a major object impacted the Earth at the time the sediment was forming, between ~600 and ~550 Ma, which is coherent with the estimated age range of the Acraman impact in Australia.

1 Introduction

The accretion of extraterrestrial material falling onto Earth can be tracked using geochemical tracers, which are more abundant and isotopically distinct in the extraterrestrial materials compared to the Earth's surface. For example, Ir concentrations, He isotopes and Os isotopes (e.g. (Peucker-Ehrenbrink 2001)) and Cr isotopes (Mougel et al., 2017) are particularly well suited geochemical tracers. Amongst those elements, He has the largest abundance variations between extraterrestrial and terrestrial material, with ^{3}He abundances and ^{3}He/^{4}He ratios in extraterrestrial material respectively ~10^9 and ~10^5 times higher than that of the Earth's crustal rocks (see review in (McGee and Mukhopadhyay, 2013)). Consequently, the measurements of He isotopes in marine sediments, or sedimentary rocks of different ages have been the subject of numerous studies for several decades, in order to track the accretion of extraterrestrial material onto Earth over geological timescales (e.g. (Amari and Ozima, 1988; Farley et al., 2006; Marcantonio et al., 1995; Murphy et al., 2010; Takayanagi and Ozima, 1987))

However, since He is an element with a high diffusivity (Hiyagon, 1994), it is likely to be partially or totally lost from the samples either during their entry into the atmosphere of after their deposition at the Earth's surface. For instance, among the extraterrestrial micrometeorites falling onto Earth, He can only be retained in the smallest ones (e.g. <10µm) because, due to their micrometric size, they experience less frictional heating during their entry in the Earth atmosphere than bigger objects (Farley et al., 1997).

Although the oldest samples with a record of extraterrestrial ^{3}He are 480 Ma old carbonates (Patterson et al., 1998), due to its high diffusivity, He is likely to be partially or totally lost during its stay at the surface for millions of years. Thus, it is interesting to focus on Ne isotopes, because Ne is less sensitive to diffusion than He. According to the diffusion experiments of (Hiyagon, 1994), Ne would be retained in IDP at typical seafloor temperatures during the transit times of the ocean crust on the seafloor, unlike He, which would be significantly released from the IDP at these temperatures over million-year timescales.

Moreover, Ne isotopes have also distinct signatures in extraterrestrial materials compared to the Earth's surface. The Ne IDP signature is close to that of the Ne-B value (12.52 ±0.18, (Black,

1972), 12.73±0.02, (Moreira, 2013; Moreira and Charnoz, 2016) and has been recently recorded in marine sediments together with IDP-derived He (Chavrit et al., 2016). Ne-B results from irradiation and sputtering processes in space (Moreira, 2013). As such, it preferentially is found in the outer 100 nm of objects and thus recovered in objects with a high surface to volume ratio such as IDP. Bigger objects such as meteorites can also include the Ne-B component if they derive from a regolith, however, they can additionally contain the Ne-A component (e.g. (Black, 1972; Pepin, 1967)), which has been recorded in pre-solar nano-diamonds (Huss and Lewis, 1994) and is particularly found in carbonaceous chondrites (see review in (Moreira, 2013)). Those two extraterrestrial signatures are distinct from the one that characterizes the material at the surface of the Earth. Combining He and Ne isotopes can allow to assess the amount of He lost from the samples (Chavrit et al., 2016). Thus, this could be used to trace the accretion of different size ranges of the extraterrestrial material falling onto Earth. Neon being less sensitive to diffusion than He, it has the potential to trace different size ranges of extraterrestrial objects accreting onto Earth (from micrometeorites to meteorites).

In this study, we coupled He and Ne isotopic measurements in samples of ~550 to ~600 Ma old sedimentary rocks from the same location in Oman in order to trace the extraterrestrial material accretion during this time period.

2 Samples and geological context

The samples are 13 limestones, dolostones and calcareous shale from the Ediacaran-aged Huqf Supergroup in Oman. Samples come from MQR-1 well and span a depth range from 3228 – 3936 m, corresponding to the Khufai, Shuram, and Buah formations of the Nafun group. The samples are believed to have been deposited in the interval between ~600 Ma to ~550 Ma (Figure 1) (Bowring et al., 2003; Condon et al., 2005; Fike et al., 2006; Grotzinger et al., 1995; Le Guerroué et al., 2006), although the middle Ediacaran interval has notoriously poor chronostratigraphic resolution, frustrating attempts to link together records of environmental and ecological change over this critical interval of Earth history.

These samples have been previously characterized for their carbon and sulfur isotopic composition (Burns and Matter, 1993; Fike et al., 2006). The data record the largest known

120 $\delta^{13}C_{carbonate}$ negative excursion in Earth history, called the Shuram excursion, which is
121 characterized by $\delta^{13}C_{carb}$ values decreasing to -12‰ (Fike et al., 2006), Figure 1).
122 The origin of this excursion is still subject to debate. The Shuram excursion was first attributed
123 to diagenetic alteration (Burns and Matter, 1993). However, methods to assess the diagenesis
124 process have failed to validate this hypothesis (Le Guerroué, 2010). In addition, this excursion
125 has been documented in multiple sites in the world, and it is more likely that the $\delta^{13}C_{carbonate}$
126 values reflect a primary signal encoded into the sediments during deposition (Fike et al., 2006;
127 Grotzinger et al., 2011 ; Le Guerroué and Cozzi, 2010).
128
129
130 **3 Methods**
131
132 **3.1 He and Ne isotopes measurements**
133
134 The sediment sample preparation is the same as in (Chavrit et al., 2016). Fractions of powdered
135 samples weighting between 0.2 and 2 g (Table 1) were decarbonated on a heating plate at 60°C
136 using 10% acetic acid. For noble gas analysis, the carbonate fraction of the samples has to be
137 removed to improve the gas purification. After three rinsing with milliQ water, each residue was
138 dried at 60°C and packed into 1 or 2 Al foil packets, allowing for the measurement of duplicates.
139 Sample 3404 was prepared twice. The packets were loaded into a sample tree made of Pyrex
140 connected to the mass spectrometer. The extraction line was baked out at ~120°C and sample
141 tree baked out at ~60°C for ~12 h during pumping prior to the measurements. The gases were
142 extracted from the samples under high vacuum using a furnace at 1200°C. After purification, the
143 ^{3}He, ^{4}He, ^{20}Ne, ^{21}Ne and ^{22}Ne were sequentially analyzed using the Noblesse mass spectrometer
144 (Nu instruments) located at the Institut de Physique du Globe de Paris (IPGP), France, following
145 the method described in (Chavrit et al., 2016). Together with an air standard for Ne, the isotopic
146 compositions of the homemade gas standard used to calibrate the data are the following:
147 $^{3}He/^{4}He=7.73\ R_A$, $^{20}Ne/^{22}Ne=9.94$, $^{21}Ne/^{22}Ne=0.0309$. On average, the furnace blank values,
148 made at a temperature of 1200°C, were 6×10^{-9} cm^3 STP for ^{4}He and 3.6×10^{-12} cm^3 STP for ^{22}Ne.
149 Seven duplicates were analyzed in order to assess the reproducibility of the measurements.
150 Duplicates of each sample were all from the same residual fraction which was split into several

Al foil packets, except for sample 3404 which aliquots 2 and 3 were from a residual fraction different from that of aliquot 1 (Table 1).

In order to understand the origin of the Ne composition of the samples, we publish data of 3 Durango fluorapatites (Table 1) analyzed in 2006 by laser heating (Yb doped fiber laser) using the ARESIBO mass spectrometer at the IPGP (Moreira and Allègre, 2002).

4 Results

The results are reported in Table 1. The non-carbonate fractions (NCF) range from 11% for the dolostone at 3428 m depth to 73% for the calcareous shale at 3722 m depth. $^{3}He/^{4}He$ ratios range between 0.006±0.003 R_A (3228#1) and 0.27±0.01 R_A (3404#2). R_A is the atmospheric ratio, with a value of 1.384×10^{-6} (Clarke et al., 1976b). The three highest $^{3}He/^{4}He$ ratios are similar and correspond to the 3 duplicates of 3404, indicating a good reproducibility of the results. ^{3}He contents range between 0.6 and 31 $\times10^{-13}$ cm^3 $STP.g^{-1}$. They are in the same range as the data from the literature on samples that show evidence for an extraterrestrial ^{3}He contribution (Figure 2). In addition, our He data show a positive correlation between the ^{3}He content and the $^{3}He/^{4}He$ ratio, confirming the mixing of an extraterrestrial IDP component and a terrestrial component in the samples. $^{3}He/^{4}He$ positively correlates with ^{4}He and ^{3}He meaning that these two isotopes contribute to the variation of the ratio, which can be related both to the contribution of radiogenic ^{4}He from the terrestrial component and to the contribution of ^{3}He from the extraterrestrial component.

$^{20}Ne/^{22}Ne$ ratios are close to or below the atmospheric ratio of 9.8 (Eberhardt et al., 1965), with the minimum values equal to 9.05±0.03 for sample 3636 (Figure 3). $^{21}Ne/^{22}Ne$ ratios show a high range of variation, going from 0.0345±0.0009 (3360#1) to up to three times the atmospheric ratio of 0.0290 (Eberhardt et al., 1965) with the data of sample 3636 ($^{21}Ne/^{22}Ne$=0.0935±0.0023).

In Figure 1, different trends are highlighted in the evolution of the NCF and the noble gases isotopic ratios over time and depth. From 3936 m to 3722 m, the NCF progressively increases from 16% to reach a maximum value of 73%. Then, the NCF follows a constant decrease down to 11% at 3428 m, followed by a relatively regular increase up to 30% at 3228 m. $^{3}He/^{4}He$ ratios

do not show a clear evolution, apart from two sharp positive peaks at 3826 m and 3404 m. $^{20}Ne/^{22}Ne$ ratios and $^{21}Ne/^{22}Ne$ ratios show an opposite evolution. Whereas $^{20}Ne/^{22}Ne$ ratios decrease progressively from 3936 m to reach a minimum value at 3636 m, the $^{21}Ne/^{22}Ne$ ratios increase. Between 3636 m and 3428 m, the $^{20}Ne/^{22}Ne$ ratios increases whereas the $^{21}Ne/^{22}Ne$ ratio decreases. At 3404 m, the $^{20}Ne/^{22}Ne$ ratios show a sharp negative spike, associated to a positive $^{3}He/^{4}He$ peak. Three duplicates of the sample at 3404 m show the same composition (Table 1) excluding a possible analytical problem during the measurement.

5 Discussion

In this part, we will highlight an unusual Ne isotopic signature. We will detail the two hypotheses that could explain such value.

5.1 The recording of an unusual Ne signature

In a $^{20}Ne/^{22}Ne$ vs $^{21}Ne/^{22}Ne$ diagram, our new data do not plot in the same area as previously analyzed terrestrial sediments (Figure 3), that showed evidence of IDP derived Ne (Chavrit et al., 2016). It does not necessarily mean that IDP are absent from the samples. More preferentially, the Ne IDP signal may be overprinted, as it is also the case for helium, because the samples contain much higher NCF than the samples of (Chavrit et al., 2016) (Annex Figure A1 of the supplementary material).

Except for the sample at 3404 m, our samples fall into the field defined by crustal fluids (Holland et al., 2013; Kennedy et al., 1990; Lippmann-Pipke et al., 2011) or by the continental crust from the KTB drill in Germany (Drescher et al., 1998). Sample 3404 presents an unusual Ne isotopic composition, with a $^{20}Ne/^{22}Ne$ ratio lower than that of the other samples at similar $^{21}Ne/^{22}Ne$ ratio and falls outside this crustal fluid field. The three analyses of the Ne isotopic composition of this sample are in excellent agreement (Table 1, Figure 3) indicating that this signature is not an analytical artifact. In order to better understand this Ne isotopic composition, we have calculated the slope of the mixing line going through each sample and the air component in the Ne three isotopes diagram. In Figure 4, these slopes do not show a progressive evolution with depth of the samples while the 3404m sample shows a strong negative spike. Consequently, this

unusual Ne isotopic signature seems to be localized and to only affect the layer at 3404 m. It corresponds to the late stage of the Shuram excursion, at a slope break where the $\delta^{13}C$ starts to recover more rapidly, at the beginning of the Buah formation (Figure 1). In the following we are going to explore the two hypotheses that could explain such composition.

5.2 A F-bearing mineral for the unusual Ne signature?

5.2.1 Neon nucleogenic production in Earth samples

In the continental crust, the radioactive decay of $^{235,238}U$ and ^{232}Th produce α particles, most of which stabilize in radiogenic ^{4}He. The other α particles react with surroundings atomic nuclei, such as ^{17}O, ^{18}O and ^{19}F isotopes to produce respectively nucleogenic ^{20}Ne, ^{21}Ne and ^{22}Ne (Figure 5). ^{20}Ne, ^{21}Ne and ^{22}Ne are also produced by neutron activation from ^{23}Na, ^{24}Mg, ^{25}Mg (Figure 5), however, these reactions account for less than 1% of the Ne production in the crust (Yatsevich and Honda, 1997). Based on the previous works of (Yatsevich and Honda, 1997) and (Hünemohr, 1989), production rates (in cm^3 STP $g^{-1}.yr^{-1}$) have been empirically quantified by (Ballentine and Burnard, 2002) as a function of the U, Th and F contents (in ppm) and O, Mg, Na contents (in wt%), with the following equations:

$$^{20}Ne\ produced\ = (6.39[U] + 0.770[Th])(0.0226[O] + 0.0022[Na]) \times 10^{-22} \quad (1)$$

$$^{21}Ne\ produced\ = \{(1.48[U] + 0.186[Th])[O] + (0.105[U] + 0.0179[Th])[Mg]\} \times 10^{-22} \quad (2)$$

$$^{22}Ne\ produced\ = \{(3.06[U] + 0.417[Th])[F] + (4.20[U] + 0.663[Th])[Mg]\} \times 10^{-24} \quad (3)$$

These equations show that the nucleogenic $^{20}Ne/^{22}Ne$ and $^{21}Ne/^{22}Ne$ production ratios are principally dependent on the O/F ratios of the samples as F in involved only on the production of ^{22}Ne. As Mg is a major element, its natural variations of concentration remain small compared to other trace elements such as F, U, Th. Variable O/F ratios will have the effect to change the slopes of the mixing lines between the atmospheric endmember and the nucleogenic endmember in a graph $^{20}Ne/^{22}Ne$ versus $^{21}Ne/^{22}Ne$ (Figure 3).

The continental crust nucleogenic trend predicted by (Yatsevich and Honda, 1997) corresponds to a O/F ratio of 752 (atomic ratio) (Ballentine and Burnard, 2002), according to the previous

equations (1), (2) and (3). Archean fluids also follow a similar trend (Holland et al., 2013). Crustal fluids data of (Kennedy et al., 1990) lie on a trend with O/F=113 (Ballentine and Burnard, 2002). Almost all data from the literature, being crustal fluids of different ages, plot in the field with an O/F ratio ranging from ~113 to ~752 (Figure 3).

After equations (1), (2) and (3), O/F ratios lower than 113 can be obtained for minerals very rich in F and/or very poor in oxygen. It is the case for a full range of accessory minerals, for example bastnäsite, containing 7.35 wt%F (O/F=4), or fergusonite (F=1.42 wt%, O/F=34) (Ballentine and Burnard, 2002; Eikenberg et al., 1993; Hünemohr, 1989). It has the consequence of significantly shifting common nucleogenic trends towards trends with more negative slopes (Figure 3). Some major minerals can also present a low O/F ratio. For example, fluorite (CaF_2), which does not contain any oxygen, is characterized by an O/F ratio of 0. Fluorapatite, the most common phosphate mineral in the environment is also characterized by a low O/F (O/F=12). Neon isotopic measurements of the Durango fluorapatite (Table 1, Figure 3) are in agreement with the nucleogenic trend defined using O/F=12, determined theoretically using the mineral formula ($Ca_5(PO_4)_3F$), suggesting that the empirical equations are reliable to estimate the $^{20}Ne/^{22}Ne$ and $^{21}Ne/^{22}Ne$ production ratios and consequently the nucleogenic trends.

5.2.2 Unusual Ne signature: a particular terrestrial nucleogenic trend?

Except one sample, our sedimentary rock samples fall into the same field as the one of crustal fluids, corresponding to an O/F ratio ranging from ~113 to ~752 (Figure 3). For these samples, the extents of the $^{21}Ne/^{22}Ne$ ratios and ^{22}Ne contents are related to the non-carbonate fraction (Annex Figure A1 of the supplementary material), an expected correlation since Ne is produced by nuclear reactions of isotopes present in the detrital fraction of the samples, containing U and Th.

On the other hand, an O/F equal to ~34 is required to explain the composition of the 3404 m deep sample (Figure 3). An O/F ratio of 34 corresponds to the fergusonite (O=40.4 wt%, F=1.42 wt%), an accessory mineral phase. However, this sample could not only be composed of this mineral, since it contains 85% carbonates (Table 1). Alternatively, it would be more probable that the singular Ne isotopic composition could be the result of a mixing between an endmember

with production ratios similar to the one fitting the literature data and all the samples from this study except at 3404 m, that is with 113≤O/F≤752 and another endmember characterized by a mineral phase with a O/F lower than 34 such as fluorapatite or fluorite characterized respectively by O/F=12 and O/F=0 (Figure 3). The Ne isotopic compositions of these two endmembers can be apprehended. The predicted crust production ratios are the following: $^{20}Ne/^{22}Ne=0.36$, $^{21}Ne/^{22}Ne=3.67$ (Yatsevich and Honda, 1997), corresponding to an O/F ratio of 752 (Figure 3). For the other endmember, we use the isotopic neon production ratios of fluorapatite ($^{20}Ne/^{22}Ne=0.0043$; $^{21}Ne/^{22}Ne=0.0458$) and fluorite ($^{20}Ne/^{22}Ne=0$; $^{21}Ne/^{22}Ne=0$) that we calculated using the elemental proportion calculated after their mineral formulae and equations (1), (2) and (3). The details of our calculations are provided in the Annex 2 of the supplementary material. After our calculations, the decrease of the O/F ratio from 752 down to 34 in order to fit the data points of sample 3404 would require the presence of 96% ^{22}Ne derived from fluorite or 98% ^{22}Ne derived from fluorapatite in the sample.

Using equations (1), (2) and (3), we estimate that for 600 Ma old fluorites and fluorapatites, the produced ^{22}Ne concentration is ~2 orders of magnitude higher than the ^{22}Ne concentration of the samples from this study. It implies that ~0.4 to 37% fluorite, depending on the U and Th content of the fluorine-bearing phase, would be sufficient to account for the Ne composition of the ~600 Ma old sample 3404. If the signal came exclusively from fluorapatite, this mineral would need to have an abundance of 0.3-16%. To evaluate the presence of F in several of the samples, we performed SEM-EDS elemental mapping for some of the residual fractions of the samples (non-carbonate fractions) including sample 3404 (See Annex 3 of the supplementary material for the details on the SEM measurements). The maps show some spots with a F-enrichment (Figure 6). It is not possible to get reliable quantification of the data because the samples were powders that were consequently not flat and Au-coated. Nevertheless, the decarbonated fraction of sample 3404 is the one which seems to visually contain the most abundant F-bearing phases amongst the 5 analyzed samples (Figure 6), particularly compared to sample 3428 which has a similar amount of non-carbonate fraction. From these observations, it is thus possible that sample 3404 has an O/F ratio lower than those of the other samples. However, a precise quantification is required to determine if its O/F ratio is low enough to explain its peculiar Ne composition. This can be assessed using theoretical calculations. The F-rich spots in sample 3404 are associated with Ca-enrichments (Figure 6, Annex Figure A2 of the supplementary material), suggesting that these

phases are fluorites. We did not see any P peak associated with F peak in the spectra that could witness the presence of fluorapatite. If we assume that all the F-rich phases in sample 3404 were fluorite, we can estimate that ~1 wt.% of fluorite is present in the ~15 wt.% of the non-carbonate fraction of sample 3404 (Table 1) analyzed with SEM-EDS (Figure 6), thus corresponding to 0.15 wt.% of fluorite in the whole-rock sample. This first order calculation gives a value too low to explain the composition of sample 3404. However, our calculations and SEM measurements are not precise enough to be definite, especially because fluorite can contain highly variable amounts of U and Th and that we did not consider any ejection factor of α particles, which is dependent on the crystal size (Gautheron et al., 2006). Measurements of fluorite crystals of different ages and sizes are needed to better evaluate the nucleogenic Ne production in this mineral, in order to definitely test whether fluorite is responsible for the peculiar Ne composition of sample 3404.

5.3 A meteoritic origin for the unusual Ne signature?

5.3.1 The Ne-A component in sedimentary rocks

In this study, the layer at 3404 m is characterized by an unusual Ne isotopic signature, with $^{20}Ne/^{22}Ne$=9.13-9.25 and $^{21}Ne/^{22}$=0.0368-0.0373 (Table 1). If this composition cannot be explained by a nucleogenic trend (see previous section, 5.2), alternatively, it could be the result of mixing three distinct components: air, "common" nucleogenic Ne and Ne-A (Figure 3). The Ne-A component is a component present in meteorites, mainly in carbonaceous chondrites (see review in (Moreira, 2013), with a distinct signature ($^{20}Ne/^{22}Ne$=8.500±0.057, $^{21}Ne/^{22}Ne$=0.036±0.001, (Huss and Lewis, 1994) compared to those of the Earth's surface, such as air and crustal fluids (Figure 3). Consequently, a $^{20}Ne/^{22}Ne$ ratio below the air value and a relatively low $^{21}Ne/^{22}Ne$ ratio in a sedimentary rock, such as in sample 3404, open the question of the presence of a meteorite component in this sample. Such a component would imply that an impact occurred on Earth at the time the sediment formed and that pre-solar nano-diamonds contained in the bolide survived the impact, allowing this volatile element and thus the Ne-A component to be trapped in the sediments. Darrah et al. measured a Ne isotopic composition in a

65 Ma old sediment from the LL-44 GPC-3 deep sea sediment core, with $^{20}Ne/^{22}Ne$=8.85 and $^{21}Ne/^{22}Ne$=0.025 (n=2), values very different from those characterizing their other samples (Darrah and Poreda, 2012). This composition is close to the Ne-A value. As evidenced from platinum group elements excesses and the presence of the large Chicxulub crater, the Earth underwent a large meteorite impact 65 Ma ago (e.g. (Alvarez et al., 1980; Hildebrand et al., 1991; Sharpton et al., 1992). Therefore, the presence of a Ne-A component in the sediments may be a witness of a major meteoritic impact. This peculiar neon isotopic signature is also associated to the highest $^{3}He/^{4}He$ ratio (~0.27Ra), although helium alone could be used to trace an impactor (Mukhopadhyay et al., 2001).

It is extremely difficult to estimate the mass fraction of presolar nanodiamonds in the samples, as this deals with concentrations in the different endmembers, which are not well constrained. However, Huss et al. (Huss and Lewis, 1994) provide a typical concentration of ^{22}Ne of ~8 10^{-6} cm^3 STP.g^{-1} for the carrier of Ne-A (pre-solar diamonds). If we assume a simple binary mixing between a terrestrial and extraterrestrial neon, we can calculate the mass fraction of extraterrestrial material in the NCF of sample 3404 as follow:

$$\beta = \frac{R_{measured} - R_{terrestrial}}{R_{diamonds} - R_{terrestrial}} \sim 0.5 = \frac{C_{diamonds}\, M_{diamonds}}{C_{measured}\, M_{measured}} \sim \frac{8\ 10^{-6}}{2\ 10^{-10}} \frac{M_{diamonds}}{M_{measured}}$$

Where R is the $^{20}Ne/^{22}Ne$ ratio. The term 0.5 is roughly estimated from Figure 3. We can therefore estimate a mass fraction of presolar diamonds carrying the neon-A signature in the NCF to be ~10 ppm. This however assumes that no neon loss has occurred and that the neon concentrations in nanodiamonds are well preserved during the impact and after. Using the $^{3}He/^{22}Ne$ of ~1 measured in presolar nanodiamonds, by Huss and Lewis (1994) we can also estimate the theoretical extraterrestrial ^{3}He within sample 3404. The calculation above suggests that half of the ^{22}Ne (~10^{-10} ccSTP/g) in the NCF should be of extraterrestrial origin and therefore the sample should contain ~10^{-10} ccSTP/g of extraterrestrial ^{3}He in the NCF. The NCF of sample 3404 contains only ~5 10^{-12} ccSTP/g of total ^{3}He, much lower than expected from neon isotope calculation, suggesting either helium was lost during the impact or after deposition.

5.3.2 Evidence of an impact at the time sample 3404 m formed?

364 The presence of a Ne-A component would imply that an object impacted the Earth and that the
365 sedimentary rock at 3404 m would have included some ejecta containing the Ne-A component
366 during its formation. This could be related to the Acraman impact. The Acraman Lake in South
367 Australia is part of a deeply eroded impact structure in South Australia (Williams, 1986, 1994)
368 with an estimated original diameter of ~40-90 km (Haines, 2005), making it one of the ten
369 largest impact structures on Earth. The presence of ice-rafted material in layers directly below
370 and above the ejecta layer related to the Acraman impact structure, suggests that the Acraman
371 impact occurred during a phase of glaciation (Gostin et al., 2010). This could possibly
372 correspond to the Gaskiers glaciation dated at ~580 Ma (Bowring et al., 2003; Pu et al., 2016)
373 using U-Pb zircon geochronology on tuffs bracketing glacial diamictites. Similarly, (Walter et
374 al., 2000) suggested an age of 578 Ma for the Acraman impact using chemostratigraphic
375 correlation. However, the Acraman impact lacks a robust isotopic age for the ejecta layers due to
376 difficulties of dating (Schmieder et al., 2015). Thus, the age of the Acraman impact can only be
377 loosely constrained in the Ediacaran period between ~541 and ~635 Ma by stratigraphic
378 bracketing (Schmieder et al., 2015).
379 The layer at 3404 m, possibly containing the signature of Ne-A component, is not directly dated.
380 Nevertheless, the age range for the Nafun group layers has been assessed through correlations to
381 other sections (Fike et al., 2006) with U–Pb zircon ages obtained on ash beds (Bowring et al.,
382 2003; Pu et al., 2016). The unconformity below the 3836 m layer, at the base of the Shuram
383 formation, probably includes the time period of the ~580 Ma Gaskiers glaciation, based on
384 stratigraphic correlation (Bowring et al., 2003; Fike et al., 2006). The recovery of the Shuram
385 excursion (3300 m) is thought to have been completed by ~550 Ma (Condon et al., 2005). Thus,
386 the sample at 3404 m should have an age between ~580 and ~550 Ma (Figure 1). However, an
387 alternative view based on thermal subsidence curves to transform stratigraphic thicknesses of the
388 Nafun Group into time suggests that the basal Shuram is ~600 Myr (Le Guerroué et al., 2006). In
389 this scenario, the base on the Buah formation, where the layer at 3404 is located, might have an
390 age of ~575-570 Ma (Le Guerroué et al., 2006), close to the Acraman impact age of 578 Ma
391 determined by (Walter et al., 2000).
392 The estimated age range for the Acraman impact is thus consistent with the estimated time range
393 for the formation of the sample at 3404 m. Thus, the presence of an impact-derived Ne-A
394 component present in this sample that would witness an impact event is possible.

However, more precise age constraints for both the Acraman impact and for the deposition of the Nafun group layers are required to confirm the validity of this hypothesis.

6 Conclusion

We have analyzed He and Ne isotopes in Ediacaran sedimentary rocks from the Nafun Group strata, Sultanate of Oman that are believed to have been deposited between ~600-580 and ~550 Ma. Extraterrestrial He is still present in these samples and is in similar amounts to that found in 3 to 480 Myr old samples. However, we were unable to detect Ne isotopic composition of interplanetary dust, unlike other data (Chavrit et al., 2016). This may be related to the higher non-carbonate fraction in these samples as compared to previously published samples. Except for one sample, the Ne isotopic composition follows a common nucleogenic trend, similar to those defined by crustal fluids from the literature and the one predicted for the continental crust. However, the other sample, from basal strata of the Buah formation, shows an unusual Ne isotopic composition that can be explained by two hypotheses.

First, a singular nucleogenic trend deviating from the common nucleogenic trend could explain the data. This would be the case if the sample contains a fluorine bearing mineral, such as fluorite or fluorapatite, in amounts ranging respectively from 0.4 to 37% and 0.3 to 16% by mass, depending on the U and Th contents of these minerals. Using SEM, we measured that the sample contains ~0.15% fluorine and calcium rich phases. However, our estimates indicate that this abundance is lower than the minimum fluorite proportion required to explain its singular Ne composition. Nevertheless, our calculations are based on theoretical predictions and greatly rely on the amount on U and Th used, which can lead to very different yields of ^{20}Ne produced after 600 Ma, and thus lead to a wide range for the required proportion of fluorine-bearing mineral contained in this singular sample.

The other alternative is that this unusual Ne isotopic composition is related to the assimilation of an extraterrestrial Ne-A component in this sample. This could be the result of a significant meteoritic impact and, if so, would indicate that this highly volatile element was not lost to the atmosphere upon the impact. This would be consistent with the Neoproterozoic Acraman impact

in Australia. However, the ages of both the impact event and the deposition of the basal Buah Formation that contains the singular Ne isotopic composition are loosely constrained and more precise ages are required to validate the impact hypothesis for the origin of the Ne signal observed here.

For the time being, it is not possible to definitely rule out or validate one of the two hypotheses. Future work will be to investigate the Ne isotopic composition of fluorine bearing minerals of different ages to better assess their nucleogenic production over time. Sedimentary rocks containing impact ejecta should also be analyzed.

Due to its signature in chondrites, Ne can potentially be an indicator of meteoritic impact in sedimentary rocks. However, this study shows that in samples that are hundreds of million years old, small amounts of F-bearing minerals can significantly affect the resulting Ne isotopic composition. Thus, it is essential to consider the nucleogenic Ne production, in deciphering the Ne isotopic composition in sedimentary rocks, especially for very old ones.

Acknowledgments

We thank the Oman Ministry of Oil and Gas for permission to publish this paper. We thank Stephan Borensztajn for assistance during with the SEM measurements and Cécile Gautheron for providing the Durango fluorapatite. FM thanks the European Research Council under the European Community's H2020 framework program/ERC grant agreement # 637503 (Pristine), the Agence Nationale de la Recherche for a chaire d'Excellence Sorbonne Paris Cité (IDEX13C445) and the Plateform PARI. FM and MM thank the UnivEarthS Labex program (ANR-10-LABX-0023 and ANR-11-IDEX-0005-02). P. Sarda, J. Hopp and the two other anonymous reviewers are thanked for their constructive reviews. This is IPGP contribution number 4027.

References

Alvarez , L.W., Alvarez, W., Asaro , F. and Michel , H.V. (1980) Extraterrestrial cause for the Cretaceous-Tertiary extinction. Science 208, 1095.

Amari, S. and Ozima, M. (1988) Extra-terrestrial noble gases in deep-sea sediments. Geochimica et Cosmochimica Acta 52, 1087-1095.

Ballentine, C.J. and Burnard, P.G. (2002) Production, Release and Transport of Noble Gases in the Continental Crust. Rev. Mineral. Geochem 47, 481-538.

Black, D.C. (1972) On the origins of trapped helium, neon and argon isotopic variations in meteorites—I. Gas-rich meteorites, lunar soil and breccia Geochimica et Cosmochimica Acta 36, 347-375.

Bowring , S., Myrow, P., Landing, E., Ramezani , J. and Grotzinger, J. (2003) Geochronological constraints on terminal Neoproterozoic events and the rise of Metazoan. EGS - AGU - EUG Joint Assembly, Abstracts from the meeting held in Nice, France, 6 - 11 April 2003 abstract #13219.

Burns, S.J. and Matter, A. (1993) Carbon isotopic record of the latest Proterozoic from Oman. Eclogae Geologicae Helvetiae 86, 595-607.

Chavrit, D., Moreira, M. and Moynier , F. (2016) Estimation of the extraterrestrial 3He and 20Ne fluxes on Earth from He and Ne systematics in marine sediments. Earth and Planetary Science Letters 436, 10-18.

Clarke, W.B., jenkins, W.J. and Top, Z. (1976a) Determination of tritium by mass spectrometric measurement of 3He. The International Journal of Applied Radiation and Isotopes 27, 512-522.

Clarke, W.B., Jenkins, W.J. and Top, Z. (1976b) Determination of tritium by mass spectrometric measurement of 3He. Int. J. Appl. radiat. Isot. 27, 515-522.

Condon, D., Zhu , M., Bowring, S., Wang, W., Yang , A. and Jin , Y. (2005) U-Pb Ages from the Neoproterozoic Doushantuo Formation, China. Science 308, 95.

Darrah, T.H. and Poreda, R. (2012) Evaluating the accretion of meteoritic debris and interplanetary dust particles in the GPC-3 sediment core using noble gas and mineralogical tracers. Geochim. Cosmoch. Acta 84, 329-352.

Drescher, J., Kirsten, T. and Schafer, K. (1998) The rare gas inventory of the continental crust, recovered by the KTB continental deep drilling project. Earth and Planetary Science Letters 154, 247-263.

Eberhardt, P., Eugster, E. and Marti, K. (1965) A redetermination of the isotopic composition of atmospheric neon. Z. Naturforsch. 20a, 623-624.

Eikenberg, J., Signer, P. and Wieler, R. (1993) U-Xe, U-Kr, and U-Pb systematics for dating uranium minerals and investigations of the production of nucleogenic neon and argon. Geochim. Cosmoch. Acta 57, 1053-1069.

Farley, K.A., Shoemaker, E.M., Montanari, A. and Patterson, D.B. (1997) Helium-3 evidence for a comet shower in the late Eocene. Seventh annual V. M. Goldschmidt conference, Tucson, AZ, United States, June 2-6, 1997 LPI Contribution, vol.921, pp.68-69, 1997.

Farley , K.A., Vokrouhlicky , D., Bottke , W.F. and Nesvorny, D. (2006) A late Miocene dust shower from the break-up of an asteroid in the main belt. Nature 439, 295-297.

Fike , D.A., Grotzinger, J.P., Pratt , L.M. and Summons, R.E. (2006) Oxidation of the Ediacaran Ocean. Nature 444, 744-747.

Gautheron, C., tassan-Got, L. and Farley, K.A. (2006) (U-Th)/Ne chronometry. Earth and Planetary Science Letters 243, 520-535.

Gostin, V.A., McKirdy, D.M., Webster, L.J. and Williams, G.E. (2010) Ediacaran ice-rafting and coeval asteroid impact, South Australia: insights into the terminal Proterozoic environment. Australian Journal of Earth Sciences 57, 859-869.

Grotzinger, J.P., Bowring , S.A., Saylor , B.Z. and Kaufman , A.J. (1995) Biostratigraphic and geochronologic constraints on early animal evolution. Science 270, 598.

Grotzinger, J.P., Fike, D.A. and Fischer, W.W. (2011) Enigmatic origin of the largest-known carbon isotope excursion in Earth's history. Nature Geosci 4, 285-292.

Haines, P.W. (2005) Impact cratering and distal ejecta: the Australian record. Australian Journal of Earth Sciences 52.

Hildebrand, A.R., Penfield, G.T., Kring, D.A., Pilkington, M., Camargo Z., A., Jacobsen, S.B. and Boynton, W.V. (1991) Chicxulub Crater: a possible Cretaceous/Tertiary boundary impact crater on the Yucatán Peninsula, Mexico. Geology 19, 867-871.

Hiyagon, H. (1994) Retention of Solar Helium and Neon in IDPs in Deep Sea Sediment. Science 263, 1257-1259.

Holland, G., Sherwood Lollar, B., Li, L., Lacrampe-Couloume, G., Slater, G.F. and Ballentine, C.J. (2013) Deep fracture fluids isolated in the crust since the Precambrian era. Nature 497, 357-360.

518 Hünemohr, H. (1989) Edelgase in U- und Th-reichen Mineralen und die Bestimmung der ^{21}Ne-
519 Dicktarget-Ausbeute der ^{18}O(a,n)^{21}Ne-Kernreaktion im Beraich 4.0 - 8.8 MeV. Johannes-
520 Gutenberg-Universität in Mainz.
521 Huss, G.R. and Lewis, R. (1994) Noble gases in presolar diamonds II : Component abundances
522 reflect thermal processing. Meteoritics 29, 811-829.
523 Kennedy, B.M., Hiyagon, H. and Reynolds, J.H. (1990) Crustal neon: a striking uniformity.
524 Earth and Planetary Science Letters 98, 277-286.
525 Le Guerroué, E. (2010) Duration and synchroneity of the largest negative carbon isotope
526 excursion on Earth: The Shuram/Wonoka anomaly. Comptes Rendus Geoscience 342, 204-
527 214.
528 Le Guerroué, E., Allen, P.A., Cozzi, A., Etienne , J.L. and Fanning , M. (2006) 50 Myr recovery
529 from the largest negative δ13C excursion in the Ediacaran ocean. Terra Nova 18, 147-153.
530 Le Guerroué, E. and Cozzi, A. (2010) Veracity of Neoproterozoic negative C-isotope values: the
531 termination of the Shuram negative excursion. Gondwana Research 17, 653-661.
532 Lippmann-Pipke, J., Sherwood Lollar, B., Niedermann, S., Stroncik, N.A., Naumann , R., van
533 Heerden , E. and Onstott , T.C. (2011) Neon identifies two billion year old fluid
534 component in Kaapvaal Craton. Chem. Geol. 283, 287-296.
535 Marcantonio, F., Kumar, N., Stute, M., Anderson, R.F., Seidl , M.A., Schlosser , P. and Mix , A.
536 (1995) A comparative study of accumulation rates derived by He and Th isotope analysis
537 of marine sediments. Earth and Planetary Science Letters 133, 549-555.
538 McGee, D. and Mukhopadhyay, S. (2013) Extraterrestrial He in sediments: from recorder of
539 asteroid collisions to timekeeper of global environmental change. in: Burnard, P.G. (Ed.),
540 The Noble Gases as Geochemical Tracers. Springer Berlin Heidelberg, 155-176.
541 Moreira, M. (2013) Noble gas constraints on the origin and evolution of earth's volatiles.
542 Geochemical Perspectives 2, 229-403.
543 Moreira, M. and Allègre, C.J. (2002) Rare gas systematics on Mid Atlantic Ridge (37°-40°).
544 Earth and Planetary Science Letters 198, 401-416.
545 Moreira, M. and Charnoz, S. (2016) Origin of the neon in Earth and in chondrites. Earth and
546 Planetary Science Letters 433, 249-256.

Mougel , B., Moynier, F., Göpel, C. and Koeberl , C. (2017) Chromium isotope evidence in ejecta deposits for the nature of Paleoproterozoic impactors. Earth and Planetary Science Letters 460, 105-111.

Mukhopadhyay, S., Farley, K.A. and Montanari, A. (2001) A short duration of the Cretaceous-Tertiary boundary event: evidence from extraterrestrial Helium-3. Science 291, 1952-1955.

Murphy, B.H., Farley , K.A. and Zachos, J.C. (2010) An extraterrestrial 3He-based timescale for the Paleocene–Eocene thermal maximum (PETM) from Walvis Ridge, IODP Site 1266. Geochim. Cosmoch. Acta 74, 5098-5108.

Patterson, D.B., Farley, K.A. and Schmitz, B. (1998) Preservation of extraterrestrial 3He in 480-Ma-old marine limestones. Earth and Planetary Science Letters 163, 315-325.

Pepin, R.O. (1967) Trapped neon in meteorites. Earth and Planetary Science Letters 2, 13-18.

Peucker-Ehrenbrink , B. (2001) Iridium and osmium as tracers of extraterrestrial matter in marine sediments. in: Peucker-Ehrenbrink, B., Schmitz, B. (Eds.), Accretion of extraterrestrial matter throughout Earth's history. Springer Science+Business Media, New York, 163-178.

Pu, J.P., Bowring, S.A., Ramezani, J., Myrow, P., Raub, T.D., Landing, E., Mills, A., Hodgin, E. and Macdonald, F.A. (2016) Dodging snowballs: geochronology of the Gaskiers glaciation and the first appearance of the Ediacaran biota. Geology.

Schmieder, M., Tohver, E., Jourdan, F., Denyszyn, S.W. and Haines, P.W. (2015) Zircons from the Acraman impact melt rock (South Australia): shock metamorphism, U–Pb and $^{40}Ar/^{39}Ar$ systematics, and implications for the isotopic dating of impact events. Geochimica et Cosmochimica Acta 161, 71-100.

Sharpton, V.L., Brent Dalrymple, G., Marin, L.E., Ryder, G., Schuraytz, B.C. and Urrutia-Fucugauchi, J. (1992) New links between the Chicxulub impact structure and the Cretaceous/Tertiary boundary. Nature 359, 819-821.

Takayanagi, M. and Ozima, M. (1987) Temporal variation of $^{3}He/^{4}He$ ratio recorded in deep-sea sediment cores. Journal of Geophysical Research 92, 12531-12538.

Walter, M.R., Veevers , J.J., Calver , C.R., Gorjan, P. and Hill, A.C. (2000) Dating the 840–544 Ma Neoproterozoic interval by isotopes of strontium, carbon, and sulfur in seawater, and some interpretative models. Precambrian Res. 100, 371-433.

577 Williams, G.E. (1986) The Acraman impact structure: source of ejecta in late Precambrian
578 shales, South Australia. Science 233, 200--203.
579 Williams, G.E. (1994) Acraman, South Australia: Australia's largest meteorite impact structure.
580 Proc. Royal Soc. Victoria 106.
581 Yatsevich, I. and Honda, M. (1997) Production of nucleogenic neon in the Earth from natural
582 radioactive decay. Journal of Geophysical Researchs 102, 10291-10298.
583
584

585 **Figure Captions**

586

587 **Figure 1:** The noble gas composition as a function of depth. NCF = non-carbonate fraction.
588 Error bars for the isotopic ratios are smaller than or equal to the symbol size when non visible.
589 The $\delta^{13}C$ carbonates data are from (Fike et al., 2006). Geochronological constraints are from
590 (Bowring et al., 2003; Condon et al., 2005; Fike et al., 2006 ; Grotzinger et al., 1995; Le
591 Guerroué et al., 2006). The Khufai and Shuram formations are separated by an unconformity
592 (wavy curve) that probably includes the Gaskiers glaciation (Bowring et al., 2003). The dotted
593 lines are the limits of the Shuram carbon isotope negative excursion (Fike et al., 2006).

594

595 **Figure 2:** $^{3}He/^{4}He$ ratio versus ^{3}He contents. The lines represent mixing lines between an IDP
596 component, rich in ^{3}He, with $^{3}He/^{4}He=2.4\times10^{-4}$ and two hypothetical terrestrial endmembers,
597 rich in radiogenic ^{4}He and poor in ^{3}He considering $^{3}He/^{4}He=10^{-9}$-10^{-7}. The 2 mixing lines are
598 derived from (McGee and Mukhopadhyay, 2013). Examples of literature data (small grey dots)
599 are from (Chavrit et al., 2016; Farley et al., 2006; Murphy et al., 2010) , and Chavrit et al.
600 (unpublished data).

601

602

603 **Figure 3:** $^{20}Ne/^{22}Ne$ ratios versus $^{21}Ne/^{22}Ne$ ratios. Sedim. stands for sediments or sedimentary
604 rocks, mfl = mass fractionation line. The plain lines are nucleogenic trends for different O/F
605 ratios (atomic ratios). Cont. crust (=continental crust predicted) is from (Yatsevich and Honda,
606 1997). The measured crustal fluids trend with a O/F=113 (Ballentine and Burnard, 2002) is
607 obtained from the nucleogenic trend defined by the crustal fluid data from (Kennedy et al.,
608 1990). The line "KTB" represents the continental crust as sampled by the KTB drill in Germany
609 (Drescher et al., 1998). The slopes of the mixing lines between the air component and the
610 nucleogenic components are a function of the O/F ratio (presented as atomic ratios here). The
611 compositions of IDP are close to that of the Ne-B value ($^{20}Ne/^{22}Ne=12.73\pm0.02$,
612 $^{21}Ne/^{22}Ne=0.0321\pm0.0001$) (Moreira, 2013), the Ne-A composition is from (Huss and Lewis,
613 1994), the air composition is from (Eberhardt et al., 1965).

614

615 **Figure 4:** Slope of the line passing through the air component and a given sample (reflecting the
616 O/F value) in the three Ne isotopes diagram (Figure 3) as a function of the depth. The unusual
617 Ne composition characterizes a negative spike at the depth 3404 m. The dotted lines indicate the
618 limits of the Shuram excursion (Figure 1).
619
620
621 **Figure 5** : Nuclear reactions producing Ne isotopes in the crust.
622
623
624 **Figure 6:** SEM-EDS mapping of the residual powders (=non-carbonate fractions, NCF) of
625 several samples from this study. All the acquisitions were done with a resolution of 467 $nm.px^{-1}$.
626
627

628 Table 1: Helium and Ne concentrations and isotopic composition of the sedimentary rocks from
629 the Huqf Supergroup and fluorapatites analyzed in this study using the Noblesse mass
630 spectrometer sited at IPGP. Durango fluorapatites were analyzed in 2006 using the ARESIBO
631 mass spectrometer sited at that time in IPGP. Helium and neon concentrations for these three
632 samples cannot be compared to other Durango analyses since these samples were baked under
633 vacuum before analysis.
634 The sample units, depths and lithologies are from (Fike et al., 2006). In the text, the samples
635 names used correspond to their depth of collection in the drill hole (2nd column of this table).
636 Dup. = duplicate. NCF=non-carbonate fractions, corresponding to residual weight/initial weight
637 ratio in percent. *For the sedimentary rocks, the loaded mass is estimated from the residual
638 fraction after leaching. R_A is the atmospheric $^3He/^4He$ ratio (1.384×10^{-6}; (Clarke et al., 1976a).
639 The concentrations are expressed in cm^3 $STP.g^{-1}$ of initial mass. Uncertainties are ±5% on
640 absolute abundances and ±2% on element ratios. #indicates the sample with the unusual Ne
641 composition.
642

643

Sample unit	Sample depth	Sample lithology	Dup.	Loaded mass*	NCF	^{4}He	^{3}He/^{4}He	σ	^{3}He/^{4}He	σ	^{22}Ne	^{20}Ne/^{22}Ne	σ	^{21}Ne/^{22}Ne	σ
						×10^{-6}	×10^{-7}				×10^{-11}				
	(m)		#	g	%				R/R$_A$						
Sedimentary rocks															
Buah	3228	silty dolostone	1	0.1567	30%	7.43	0.08	0.04	0.006	±0.003	5.31	9.45	±0.03	0.0497	±0.0012
			2	0.1428	30%	5.33	0.48	0.05	0.035	±0.004	5.51	9.39	±0.03	0.0477	±0.0012
Buah	3320	silty dolostone	1	0.1449	25%	7.22	0.92	0.07	0.067	±0.005	8.77	9.79	±0.03	0.0369	±0.0007
			2	0.0891	25%	6.57	1.09	0.08	0.079	±0.006	8.10	9.76	±0.03	0.0365	±0.0007
Buah	3360	dolostone	1	0.1135	23%	1.59	2.19	0.14	0.158	±0.010	5.59	9.79	±0.03	0.0345	±0.0009
			2	0.0987	23%	1.99	1.11	0.14	0.081	±0.010	6.64	9.81	±0.03	0.0350	±0.0009
Buah	3404#	dolostone	1	0.1092	13%	1.58	2.97	0.16	0.214	±0.011	2.35	9.25	±0.03	0.0370	±0.0008
			2	0.1409	16%	1.46	3.79	0.19	0.274	±0.013	2.37	9.13	±0.03	0.0368	±0.0009
			3	0.1905	16%	1.59	2.92	0.13	0.211	±0.009	2.32	9.14	±0.03	0.0373	±0.0009
Buah	3428	dolostone	1	0.0623	11%	1.11	1.62	0.07	0.117	±0.005	2.11	9.65	±0.03	0.0401	±0.0010
Shuram	3480	silty limestone	1	0.1514	19%	3.31	0.52	0.15	0.037	±0.011	5.00	9.55	±0.03	0.0414	±0.0008
Shuram	3556	silty limestone	1	0.1556	31%	2.49	1.20	0.02	0.086	±0.002	5.04	9.34	±0.07	0.0777	±0.0013
			2	0.1892	31%	3.40	1.33	0.03	0.096	±0.002	4.81	9.45	±0.03	0.0788	±0.0005
Shuram	3636	silty limestone	1	0.1534	48%	18.13	0.73	0.12	0.052	±0.009	8.13	9.05	±0.03	0.0935	±0.0023
Shuram	3722	calcareous shale	1	0.1543	73%	21.02	0.91	0.07	0.066	±0.005	10.42	9.34	±0.03	0.0898	±0.0022
Shuram	3780	silty limestone	1	0.1031	52%	8.41	1.14	0.02	0.082	±0.001	6.79	9.49	±0.07	0.0782	±0.0016
Shuram	3826	limestone/sandstone	1	0.1476	45%	10.98	2.82	0.07	0.204	±0.005	7.76	9.56	±0.03	0.0551	±0.0014
Khufai	3900	dolostone	1	0.1297	31%	6.19	1.05	0.02	0.076	±0.002	8.71	9.73	±0.07	0.0480	±0.0008
			2	0.1956	31%	1.70	1.01	0.02	0.073	±0.002	2.75	9.65	±0.07	0.0486	±0.0008
Khufai	3936	limestone	1	0.1544	16%	7.89	0.93	0.05	0.067	±0.004	14.69	9.81	±0.01	0.0356	±0.0001
Durango fluorapatite															
DUR3-1				0.012		120					25.20	9.19	±0.07	0.0310	±0.0017
DUR4-2				0.010		100					2.88	8.05	±0.23	0.0316	±0.0034
DUR5-3				0.014		150					2.59	2.90	±0.30	0.0349	±0.0035

644

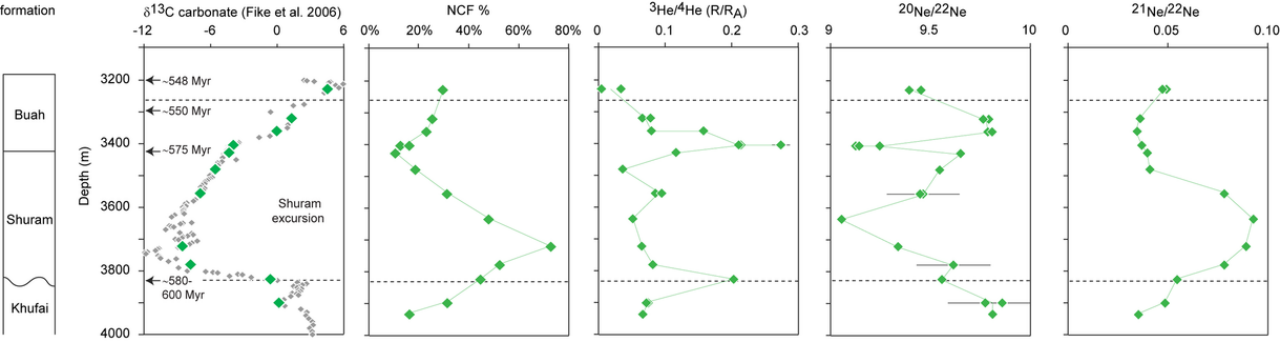
formation
Buah
Shuram
Khufai
δ13C carbonate (Fike et al. 2006)
-12
-6
0
6
NCF %
0%
20%
40%
60%
80%
3He/4He (R/RA)
0
0.1
0.2
0.3
20Ne/22Ne
9
9.5
10
21Ne/22Ne
0
0.05
0.10
Depth (m)
3200
3400
3600
3800
4000
~548 Myr
~550 Myr
~575 Myr
~580-
600 Myr
Shuram
excursion

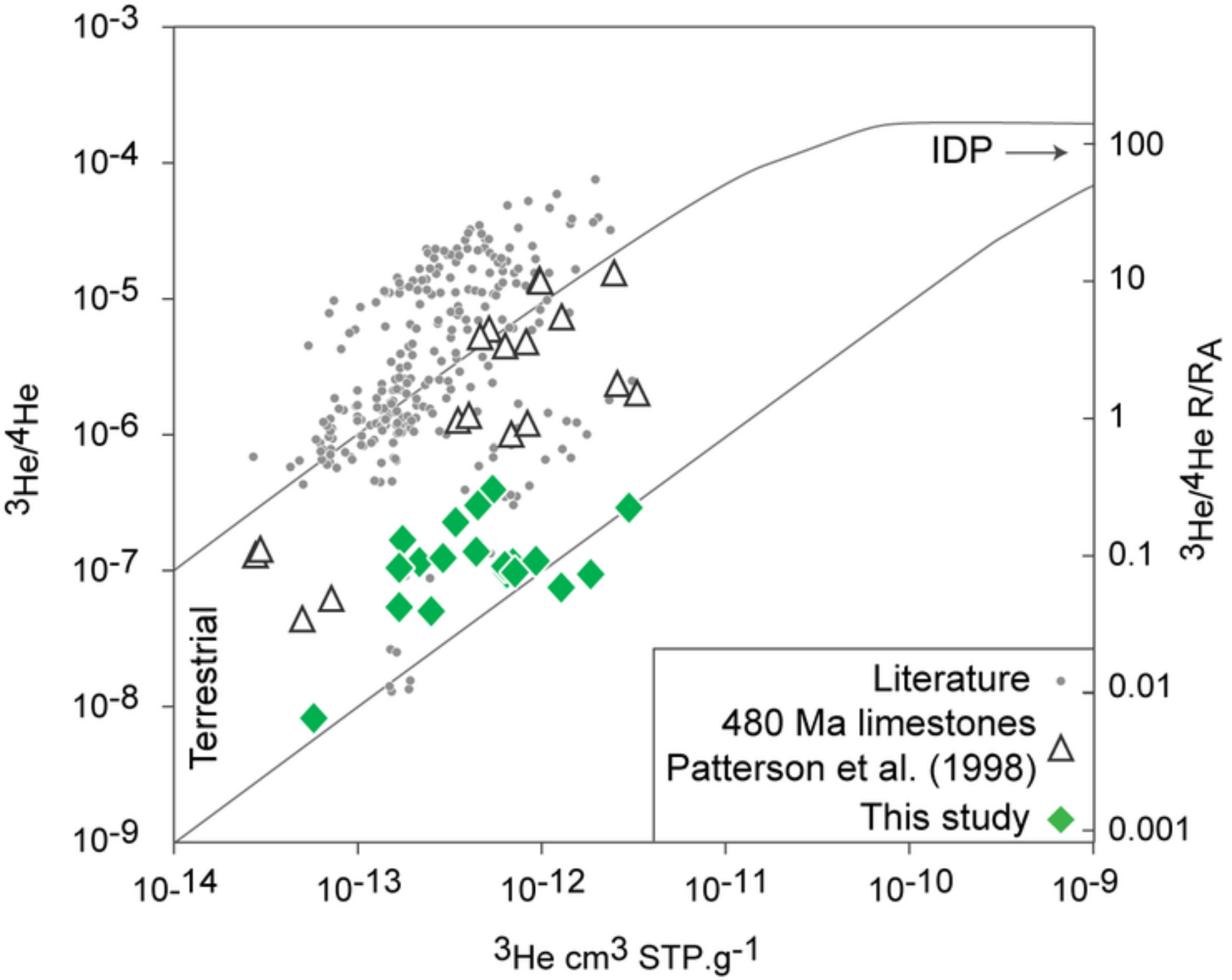
IDP
Terrestrial
Literature
480 Ma limestones
Patterson et al. (1998)
This study
$^3He/^4He$
$^3He/^4He$ R/R_A
^3He cm^3 STP.g^{-1}
10^{-3}
10^{-4}
10^{-5}
10^{-6}
10^{-7}
10^{-8}
10^{-9}
100
10
1
0.1
0.01
0.001
10^{-14}
10^{-13}
10^{-12}
10^{-11}
10^{-10}
10^{-9}

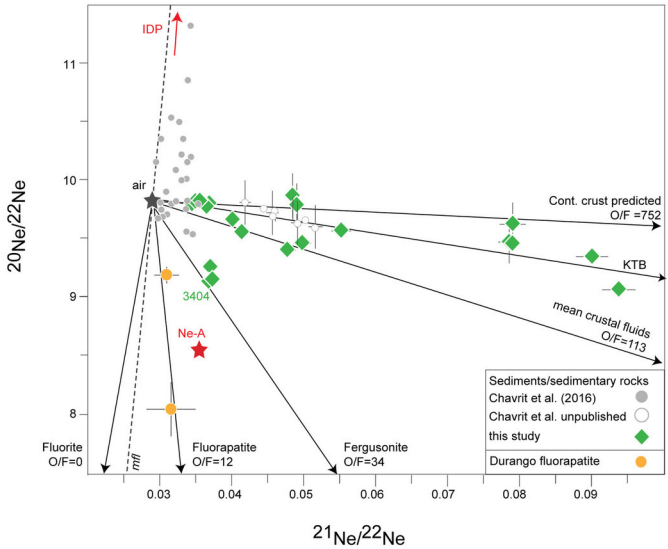
IDP
air
Cont. crust predicted
O/F =752
KTB
mean crustal fluids
O/F=113
3404
Ne-A
Fluorite
O/F=0
mlf
Fluorapatite
O/F=12
Fergusonite
O/F=34
Sediments/sedimentary rocks
Chavrit et al. (2016)
Chavrit et al. unpublished
this study
Durango fluorapatite
11
10
9
8
0.03
0.04
0.05
0.06
0.07
0.08
0.09
20Ne/22Ne
21Ne/22Ne

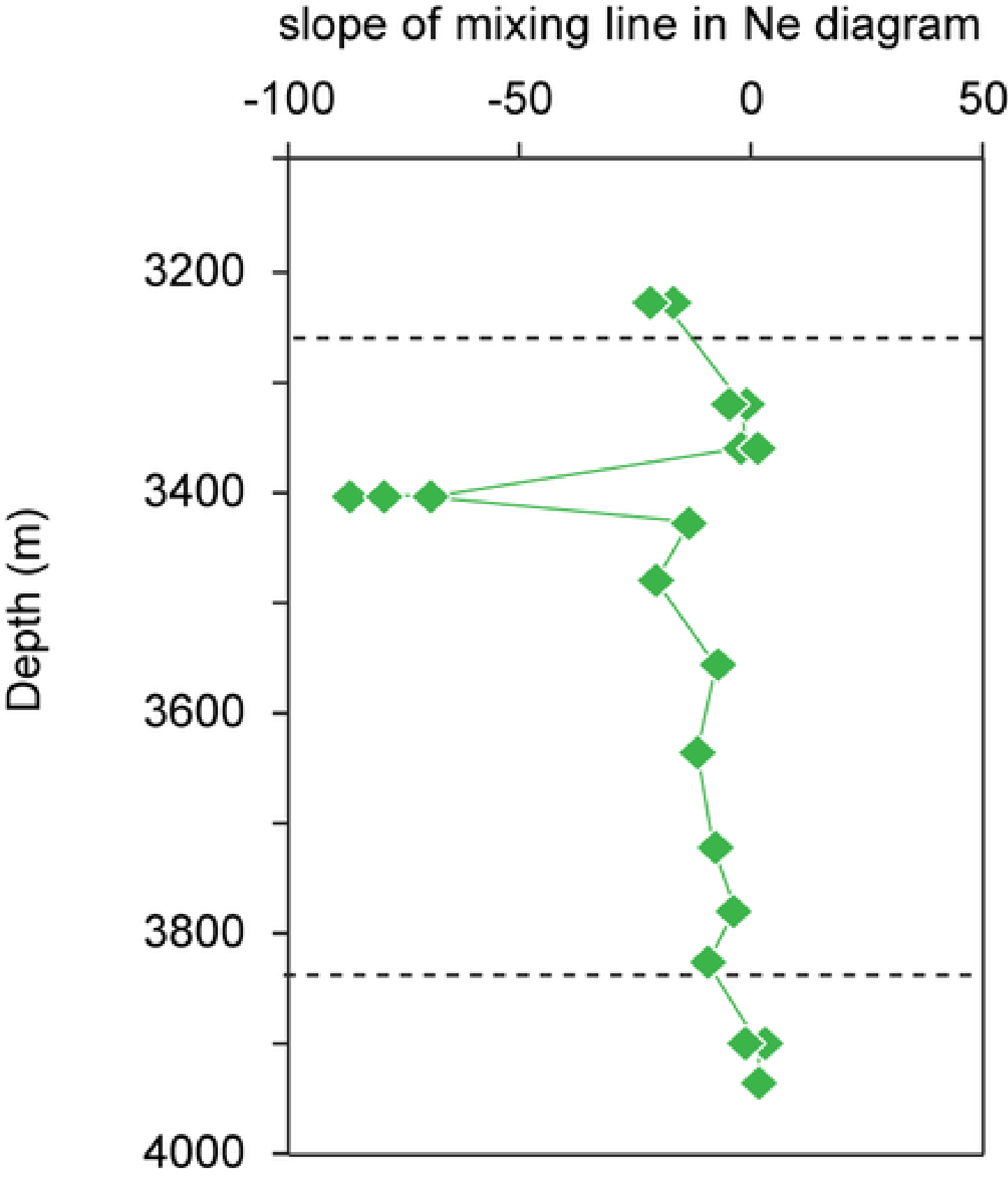
slope of mixing line in Ne diagram
-100
-50
0
50
3200
3400
3600
3800
4000
Depth (m)

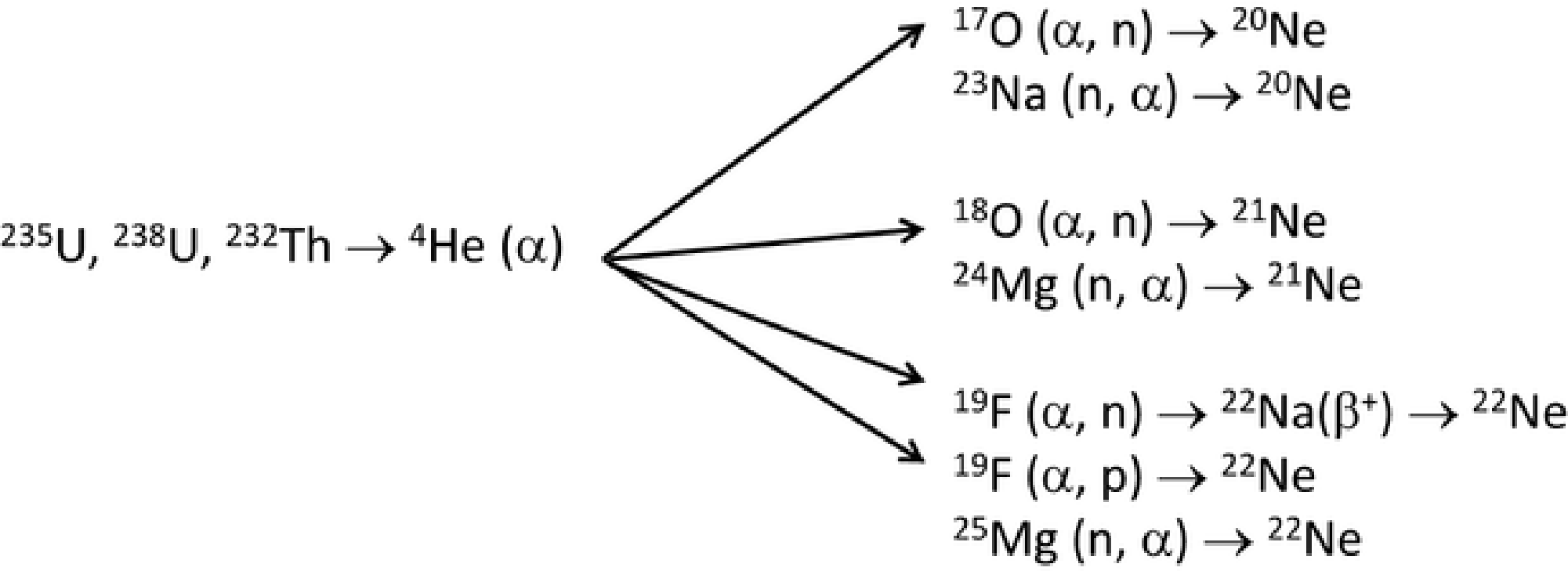
^{235}U, ^{238}U, $^{232}Th \rightarrow {}^{4}He\ (\alpha)$
$^{17}O\ (\alpha, n) \rightarrow {}^{20}Ne$
$^{23}Na\ (n, \alpha) \rightarrow {}^{20}Ne$
$^{18}O\ (\alpha, n) \rightarrow {}^{21}Ne$
$^{24}Mg\ (n, \alpha) \rightarrow {}^{21}Ne$
$^{19}F\ (\alpha, n) \rightarrow {}^{22}Na(\beta^{+}) \rightarrow {}^{22}Ne$
$^{19}F\ (\alpha, p) \rightarrow {}^{22}Ne$
$^{25}Mg\ (n, \alpha) \rightarrow {}^{22}Ne$

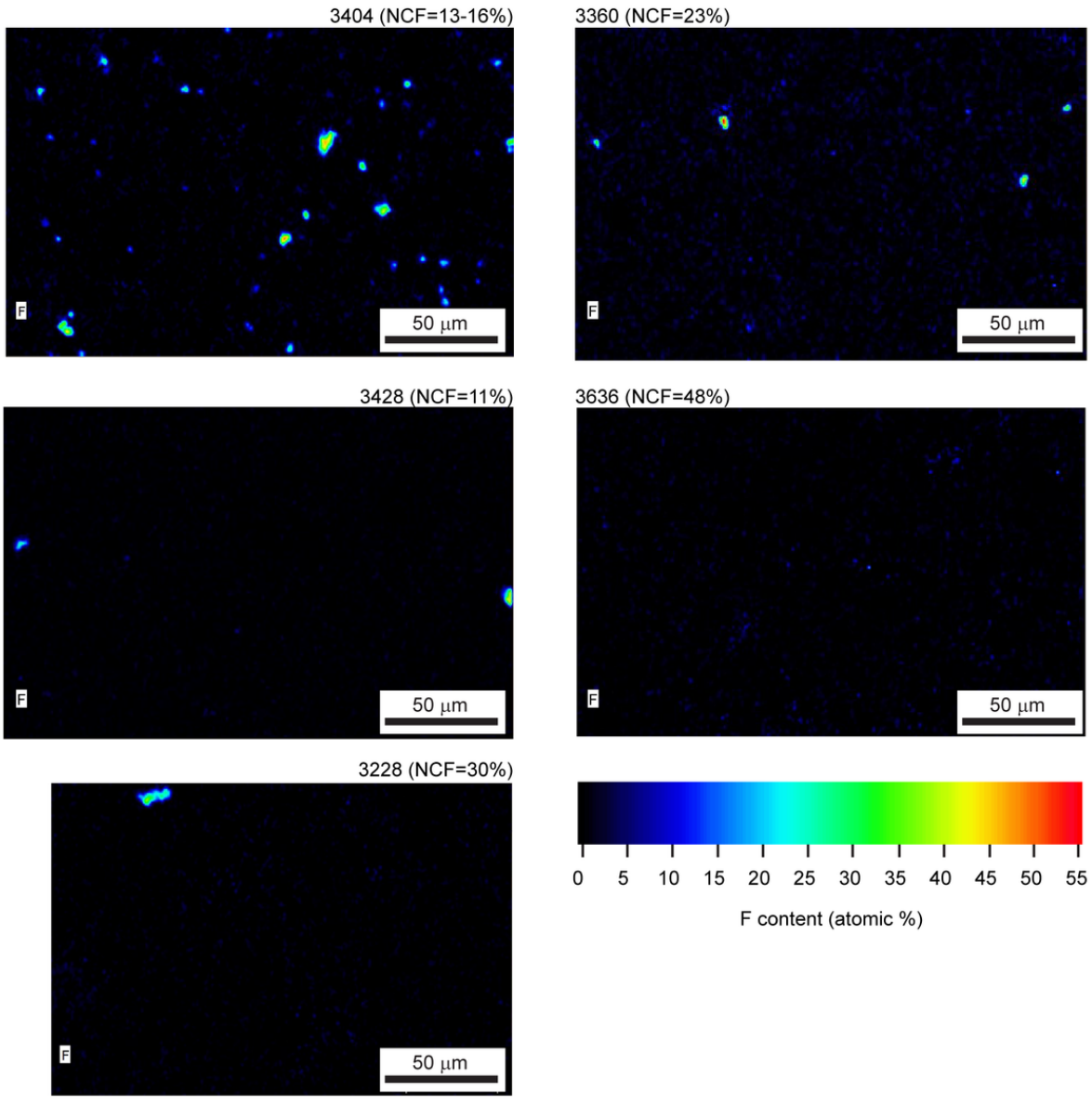
3404 (NCF=13-16%)
3360 (NCF=23%)
3428 (NCF=11%)
3636 (NCF=48%)
3228 (NCF=30%)
F
50 μm
0 5 10 15 20 25 30 35 40 45 50 55
F content (atomic %)